Low Temperature Physics/Fizika Nizkikh Temperatur, 2020, v. 46, No. 6, pp. 699–709

Interplay of hopping conductivity and superconductivity in magnetic superconductor $RuSr_2(Eu_{1.5}Ce_{0.5})Cu_2O_{10-\delta}$

E.Yu. Beliayev, V.A. Horielyi, and Yu.A. Kolesnichenko

B. Verkin Institute for Low Temperature Physics and Engineering of the National Academy of Sciences of Ukraine
47 Nauky Ave., Kharkiv 61103, Ukraine
E-mail: beliayev@ilt.kharkov.ua

Received December 11, 2019, published online April 24, 2020

In this work, we analyze the temperature dependencies of resistance and magnetoresistance for two $RuSr_2(Eu_{1.5}Ce_{0.5})Cu_2O_{10-\delta}$ ceramic samples, one of which was left in the as-prepared state while another one was oxygen saturated. The measurements on these samples were made soon after preparation and repeated after their long storage (10 years) in an ambient atmosphere when they lost most of their over-stoichiometric and part of stoichiometric oxygen. Having studied the widest possible range of oxygen concentrations, we are trying to clarify not only the questions of stability of superconducting state in ruthenocuprates, but also the interplay of various types of electronic hopping conductivity and superconductivity in granular magnetic material. Despite the significant progress made in understanding the properties of disordered conductors, the old question of mutual influence and competition between localization and superconductivity still not clear. Investigation of the properties of electron transport as it approaches the metal–insulator transition will be useful and important.

Keywords: ruthenocuprates, ferromagnetism, hopping conduction, superconductivity.

1. Introduction

For many years, superconducting ruthenocuprates with chemical composition $RuSr_2(Re_{1.5}Ce_{0.5})Cu_2O_{10-\delta}$ (where Re — usually Gd, Eu, Sm) attracted the researchers' attention by a unique combination of superconducting and magnetic properties. The coexistence of superconducting and weak ferromagnetic (WFM) states in a single crystal unit cell was confirmed in a number of experiments including scanning tunneling spectroscopy [1], Raman spectra [2] and muon spin rotation experiments [3].

Currently the scientific community has come to conclusion that superconducting state in ruthenocuprates survives due to the following scenario. Weak ferrimagnetic component $H_\perp \approx 0.1$ T [4] arises from the mutual skew of the adjacent G-type antiferromagnetically ordered moments of Ru^{+5} ions as the temperature drops down to T_m, — the temperature of the magnetic transition. It locally lowers the superconducting order parameter, but proves to be incapable of hindering germination of superconductivity in mixed state in CuO_2 layers.

This is facilitated by the elongated dimensions of the crystal unit cell along the c axis ($a = b = 3.84$ Å, $c = 28.72$ Å) that effectively separates the magnetic layers RuO_2 (the saturation moment at 5 K is $M_{sat} = 0.89$ μ_B/Ru [5]) and superconducting CuO_2 layers [6]. Also we should note huge values of the upper critical field $H_{c2} \approx 28$–80 T in these series of compounds [4]. As a result, the superconductivity in CuO_2 layers, being pierced by the ordered lattice of magnetic vortices, coexists in thermodynamic equilibrium with weak ferrimagnetic order. This order arises in the form of a spontaneous vortex phase which leads to local lowering of the superconductor order parameter but still cannot suppress it completely.

The possibilities of practical application and investigation of electron transport properties in ruthenocuprates are substantially limited by the instability of the samples and extremely small sizes of single crystals obtained. In most cases, the ruthenocuprate samples available for study in the form of sintered ceramics and their properties are strongly dependent on the degree of oxygen saturation. For the high-T_c cuprates it is well known that under such conditions most grains are coupled by weak Josephson currents forming a 3D Josephson network.

The possible nonuniformity in the phase composition should also be taken into account. The phase diagram for any compound synthesized from 6 components is obviously complex. The slightest deviations in local concentrations and the conditions of synthesis can lead to formation of new phases at the joints of grains and in the spaces between

them. The variety of phase composition in ruthenates is described in [7]. Among these an exotic triplet superconductor Sr_2RuO_4, non-fermi liquid metals $Sr_3Ru_2O_7$ and $SrRuO_3$, and magnetic superconductor $RuSr_2(Eu_{1.5}Ce_{0.5})Cu_2O_{8-\delta}$ with $T_c \approx 16$ K.

Being, in fact, high-temperature superconductors (HTSC) based on copper oxide layers, ruthenocuprates with their sophisticated chemical composition and complex crystal structure have inherited in the most aggravated extent a tendency of all copper oxide high-temperature superconductors to lose the stoichiometric oxygen included in their crystal lattice, which leads to degradation of their superconducting properties. At the same time the hopping conductivity is also profoundly affected by oxygen content. In granular ceramic samples where intragrain and intergrain properties are superimposed both of these phenomena contribute to resulting conductivity and their interplay may be of interest for clarifying the mechanisms of appearance of superconductivity and stability of superconducting state. In this sense, samples that are maximally saturated with oxygen under high pressure and gradually losing it over time are of interest as an object for studying the relationship between superconducting and dielectric states in a granular material. In order to study the interconnection of superconductivity and hopping conductivity in the widest possible range of oxygen concentration, we repeated studies of the two europium based ruthenocuprate ceramic samples after they were stored for 10 years under room conditions in ambient atmosphere.

Transition from antiferromagnetic (AFM) to the WFM state in ruthenocuprates is due to the fact that the lengths of Cu–O and Ru–O covalent bonds, being almost equal at room temperature, have different temperature dependences. With lowering temperature, the Cu–O bonds shrink more. And Ru–O bonds become too big to fit the lattice. This leads to coordinated rotation of adjacent oxygen octahedra in which the antiferromagnetically ordered Ru^{+5} ions are confined [8]. This rotation achieves the angle 14° and through Dzyaloshinskii–Moriya interaction causes the coordinated tilting of neighboring antiferromagnetically ordered Ru^{+5} magnetic moments and the weak ferrimagnetic component perpendicular to the layered structure arises in the compound. This magnetic transition manifests itself as a kink on the temperature dependence of the sample resistance at temperature $T_m \sim 135$–145 K (depending on composition). Taking into account the multivalence nature of ruthenium, which is responsible for the sophisticated magnetic properties it also seems interesting to know does this transition will be affected by the oxygen loss.

2. Experimental procedure

The test samples were prepared in the Racah Institute of Physics (The Hebrew University of Jerusalem, Israel) by solid-phase synthesis and were initially differed in oxygen content. One of the samples was left in the original (as prepared) state (sample Eu_A) while another one was annealed for 24 h at the temperature $T = 900$ °C and high pressure of pure oxygen $P = 100$ atm (sample Eu_B) [9]. The x-ray powder diffraction (XRD) studies confirmed the purity and prevailing single-phase composition (~ 97%) for the samples obtained. The unit cell parameters ($a = b = 3.846$ Å, $c = 28.72$ Å) within the experimental error coincided with the data for europium ruthenocuprates given in the works of other authors [10].

For electrical measurements the ceramic tablets were cut in pieces having the form of parallelepipeds with dimensions 10×2×1 mm by slowly rotating diamond cutter. The electrical contacts were made by vacuum silver deposition with silver glue over it. The distances between the potential contacts were 7 mm.

The measurements of $\rho(T,H)$ dependences for these two samples were carried out at the B. Verkin Institute for Low Temperature Physics and Engineering of NAS of Ukraine (Kharkiv, Ukraine) in the temperature range 3.5–350 K by 4-probe dc technique in most cases applying the current $I = 100$ μA. We were trying to select the measuring current in the region of linearity of the current-voltage characteristic (Fig. 1).

The samples were mounted on a copper sample holder in a vacuum chamber of the home-made cryostat. To improve the thermal contact the heat-conducting glue was used. The temperature in the cryostat was controlled by automatic stabilization system with accuracy from ~ 10^{-4} K in the region of liquid helium temperatures to ~ 10^{-1} K at the maximum achievable temperature of 350 K. In the experimental setup we used a stabilized dc power supply with alternating polarity to compensate for the thermal EMF, calibrated Pt and RuO_2 resistive thermometers, multimeters Keithley 2000 and nanovoltmeter Keithley 2182. Magnetoresistive studies were performed with the same experimental setup, using rotating Kapitsa's solenoid generating magnetic fields up to $H = \pm 1.0$ T applied in all these experiments perpendicular to the transport current.

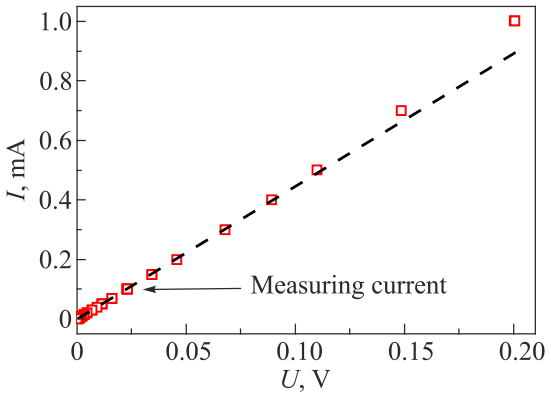

Fig. 1. Current-voltage characteristic at $T = 4.2$ K for the sample Eu_A after 10 years of storage.

3. Experimental results

3.1. ρ(T) dependences for as prepared and oxygen saturated samples

At low-temperature region where superconductivity coexists with WFM state the granular structure of initially prepared ceramic samples manifested itself in the typical "shouldered" form of the observed intragranular and intergranular superconducting transitions. As it was pointed out in [11] granular HTSCs exhibit a classical two-phase system: a set of two different second-order superconductors: three-dimensional superconducting grains with strong superconductivity and two-dimensional grain interfaces, i.e., Josephson "weak links" with weak superconductivity. The temperature dependences of resistance and corresponding derivatives $d\rho(T)/dT$ that allow us to see the intragranular and intergranular superconducting transition temperatures for two initially measured samples (Eu_A and Eu_B) are shown in Fig. 2(a), (b).

Due to the fact that the HTSC ceramic samples studied were granular systems, for the freshly prepared samples the transition to the superconducting state occurred through a two step process. For $T < 50$ K in Fig. 2(a) with decreasing temperature at first we can see the establishing of superconducting state for the substance within the granules. The critical temperatures of that transition varied in the range from $T_{cg} = 38.6$ to 45.4 K depending on the degree of oxygen saturation. Then there follows a small "shoulder", after which we can see a further drop in the resistance behavior. This new fall is associated with the establishment of Josephson weak links in the disordered intergranular material, with critical temperatures that vary from $T_{c0} = 10$ K for the "as prepared" sample Eu_A to $T_{c0} = 19.2$ K for the oxygen saturated sample Eu_B that was annealed in pure oxygen at pressure $P = 100$ atm.

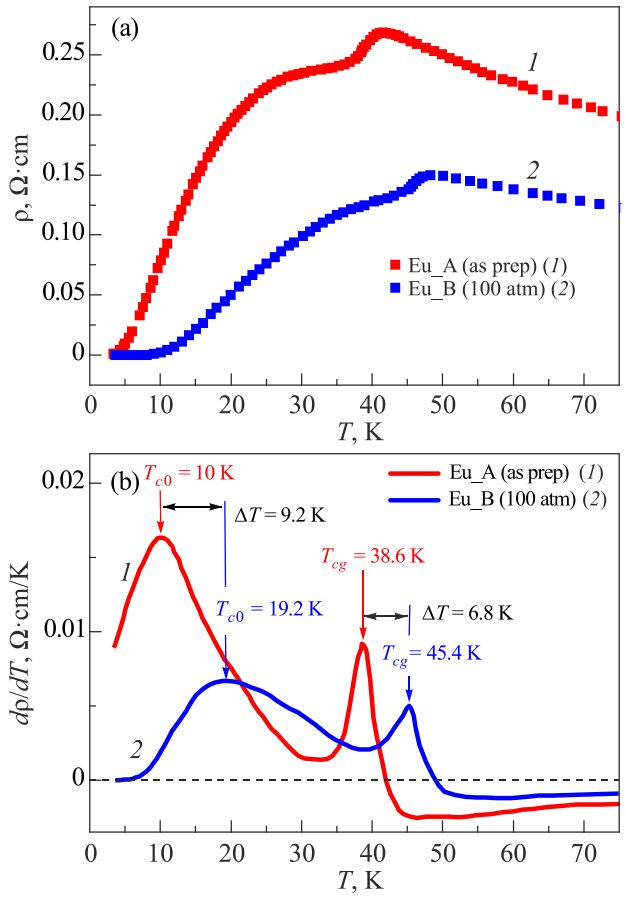

Fig. 2. (Color online) Superconductivity in initially prepared $RuSr_2(Eu_{1.5}Ce_{0.5})Cu_2O_{10-\delta}$ ceramic samples with different oxygen content (Eu_A and Eu_B): ρ(*T*) dependences for as prepared samples (a), $d\rho/dT$ derivatives to determine inter- and intragranular superconducting transition temperatures (b).

If now we consider the ρ(*T*) behavior for the as prepared samples from the side of high temperatures, (Fig. 3), for each sample for the temperature dependence of resistance we should note two regions of compliance with 3D Mott's intergranular variable range hopping (VRH) law

$$\rho \approx \rho_0 \exp\,(T_0 / T)^{1/4}, \qquad (1)$$

one of which corresponds to the electron hopping between the ruthenocuprate granules, when the intergranular substance is in the state of the AFM insulator (this law is well obeyed in the temperature interval from $T = 350$ K down to $T_m = 135$ K that, as it is known from previously published magnetic studies, corresponds to the AFM ⇒ WFM magnetic transition) while another one for the Mott's VRH conductivity between the same granules, but now being in WFM state. I.e., for the temperatures near T_m on the ρ(*T*) dependence plotted in the Mott's coordinates we observe a kink, after which in the intermediate temperature range $T = 50$–135 K we again observe 3D variable range hopping Mott's behavior, but now with a changed slope. These Mott's dependences are clearly seen in Fig. 3.

We assume that the above mentioned decrease in the slope of the $\rho(T^{-1/4})$ curve at the temperature T_m and the corresponding decrease in the Mott's temperature T_0 in Eq. (1) are associated with an increase in ferromagnetic correlations and reinforcement of the magnetic ordering in the substance. That leads to leveling the electron spins in

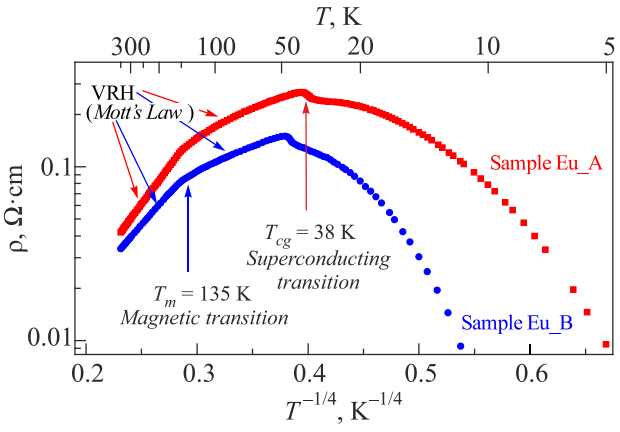

Fig. 3. VRH conductivity behavior in as prepared samples.

the neighboring granules thereby making it easier for the electrons to find a suitable state with equivalent energy and spin configuration for making a jump. The computer fitting for $\rho(T)$ curves, shown in Fig. 3 at the sections corresponding to VRH conductivity gives for the sample Eu_A the Mott's temperature T_0 = 153820 K in AFM state and $T_0' = 2550$ K in WFM state. For the sample Eu_B we have T_0 = 74400 K and $T_0' = 1385$ K respectively.

Such a decrease in Mott's temperature (assuming the immutability of the density of states at the Fermi level $g(E_F)$) according to the formula [12].

$$T_0 = \frac{A_3}{g(E_F)a^3 k_B}, \qquad (2)$$

(where A_3 — a numerical coefficient that depends on the system dimensionality; k_B — Boltzmann's constant) corresponds to the increase in the radius of localization of the charge carriers a after establishing the weak magnetic order as a factor of $\sqrt[3]{T_0'/T_0} \approx 3.75$–$3.9$. We believe that such a change in the slopes of $\rho = f(T^{-1/4})$ dependences and Mott's temperatures is associated with the ferromagnetic correlations in the contacting grains due to the increase in the magnetic ordering. This leads to the alignment of the electron spins in the adjacent granules and thus facilitates the resonant tunneling transition of charge carriers between them. In pressed sintered powders, each granule usually has 4 nearest contacting neighbors.

Based on the Mott's temperatures obtained, we can calculate the corresponding carriers' localization radii using the formula (2). Such calculations, however require the knowledge of the density of states at the Fermi level $N(E_F)$ which in our case had not been directly measured. Using the methodology proposed in the paper [13], we can estimate $N(E_F) = 2.8\cdot10^{46}$ J$^{-1}\cdot$m^{-3} and then, for the initially prepared samples with T_0 = 153820 K, we get the calculated carrier localization radius $a = 1/\sqrt[3]{N(E_F)k_B T_0}$ = = $(2.8\cdot10^{46}$ J$^{-1}\cdot$m^{-3} * $1.38\cdot10^{-23}$ J$\cdot$K^{-1} * 153820 K$)^{-1/3}$ = = 550 nm. That does coincide with the initial grain size in our ceramic samples according to TEM studies.

It should also be noted that for the freshly prepared samples in low temperature region the application of a weak magnetic field ($H \cong 0.1$ T) easily suppresses superconductivity in disordered intergranular medium but with virtually no effect on the intragranular superconducting transition. To save space we don't give corresponding curves and explanations, simply referring to similar studies performed earlier in our laboratory on the samples of gadolinium based ruthenocuprates $RuSr_2(Gd_{1.5}Ce_{0.5})Cu_2O_{10-\delta}$ [14].

Thus, the overall temperature behavior of resistance for the freshly prepared ceramic samples can be satisfactorily described by the combination of the Mott's VRH hopping mechanism for the high-temperature region and by the mechanism of intra-granular and intergranular superconducting transitions in a granular superconductor at low temperatures.

3.2. Changes in dielectric properties associated with the loss of stoichiometric oxygen

In Fig. 4 the global comparison for the temperature dependences of the resistance for the freshly prepared samples and for the same samples after 10-year storage is shown in Mott's coordinates.

First of all the measurements show that the loss of stoichiometric oxygen does not affect the temperature of the magnetic transition, which is still equals to T_m = 135 K. It is known that the magnetic properties in ruthenocuprates are determined by the magnetic moments of the Ru^{5+} ions, located in the octahedral environment of oxygen atoms. Thus, it can be assumed that, despite the fact that Ru is a variable-valence element, there is no loss of stoichiometric oxygen in its octahedral environment. This is also confirmed by the fact that RuO_2 is a fairly chemically stable oxide, used in particular in the production of highly stable resistors. So we can conclude that the oxygen depletion is closely connected with the variable valence of cerium that is partially replacing europium in Eu–Ce–O_2 fluorite-structure blocks which play the role of a dielectric spacer located between the superconducting layers of CuO and magnetically ordered layers of RuO in crystal lattice of ruthenocuprates.

Also we can see that the depletion of stoichiometric oxygen leads to a dramatic increase in the samples' resistance. But before we continue the discussion on the effect of oxygen depletion, let us analyze how the oxygen saturation affects the superconductivity, i.e., let's go back to Fig. 2.

From this picture we can conclude that in the result of oxygen saturation, the shift of superconducting transition temperature for the intergranular medium was ΔT_{ci} = 9.2 K, and for the substance inside the superconducting granules ΔT_{cg} = 6.8 K. This difference is apparently due to the mechanism of oxygen diffusion along the grain boundaries

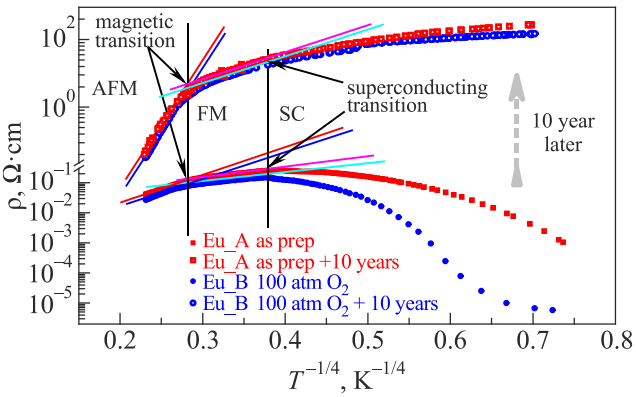

Fig. 4. (Color online) VRH and evolution of conductivity behavior with temperature and time.

where ΔT is higher. And we believe that the large width of superconducting transition for the intergranular medium (with a peak half-width of $d\rho/dT \approx 18$ K) is due to its strong inhomogeneity.

Although initially prepared samples according to XRD studies were predominantly (~ 97%) single-phase, however, there undoubtedly contained another phase — a disordered intergranular substance with very different (2–4 times lower) superconducting transition temperature (see Fig. 2).

Looking at the increased steepness of $\rho(T)$ dependence in Mott's coordinates for the samples subjected to the long-term storage (Fig. 4), it can be assumed that the intragranular substance losing oxygen over time continue to undergo phase separation. As a result each $RuSr_2(Eu_{1.5}Ce_{0.5})Cu_2O_{10-\delta}$ granule turned out to be surrounded by a thickened strongly inhomogeneous shell with lowered T_c and a large T_c spread. This shell may also contain an admixture of $RuSr_2EuCu_2O_{8-\delta}$ which is also "magnetic superconductor" with $T_c \cong 20$ K. At high temperatures, this disordered medium, with its insulating properties, led to a significant increase in the dielectric properties of the aged samples.

Returning to Fig. 4, we see that in the high-temperature region the conductivity behavior as before is determined by 3D variable range hopping, but now with a new ~ 20-fold increased Mott's temperature values $T_0' = 5975000$ K (for the sample Eu_B) and $T_0'' = 3643000$ K (for the sample Eu_A). This indicates a strong heterogeneity of the aged samples. And 20-fold increased Mott's temperature values T_0' and T_0'' mean $\sqrt[3]{20}$ decreased localization radii. Therefore, we assume that many of $RuSr_2(Eu_{1.5}Ce_{0.5})Cu_2O_{10-\delta}$ granules cracked with the formation of small tunnel gaps between their fragments. For ruthenocuprates in which the crystal lattice is a natural layered system of superconducting (CuO) and magnetic (RuO) layers separated by dielectric layers $(Ce_x\text{-}Eu_{2-x})$–O_2 with a fluorite-like structure such delamination (splitting) in the process of oxygen loss in dielectric layers seems highly likely. And this confidence is supported by the previously noted fact that the invariance of the antiferromagnetic transition temperature indicates the mechanism of oxygen loss, which is associated apparently with the variable valence of Ce atoms.

But after AFM → WFM magnetic transition we can see that the slopes of the curves for the temperature dependences of the resistance and the corresponding values of the Mott's temperatures turn out to be almost the same and approach those for the initially prepared samples. This suggests that the role of weak magnetic ordering is to align electron spins in fractured grains, which led to increasing in the probability of resonant tunneling between their fragments and to restoring of their electric integrity.

By the way, delamination of the $RuSr_2(Eu_{1.5}Ce_{0.5})Cu_2O_{10-\delta}$ granules and increase in the thickness of the disordered dielectric substance on the grain's surfaces suggests that the samples studied should exhibit strong nonlinear effects in their conductivity.

3.3. Nonlinear effects in conductivity

Before making all other measurements we have measured the current-voltage characteristic (CVC) which seemed to be linear (see Fig. 1) and choose the measurement current not too high to avoid overheating and not too low to achieve an acceptable accuracy. But analyzing the conducting state of our samples consisting of granules connected by a weak superconducting percolation network, we return to Fig. 1 and rearrange it in the coordinates $R = U / I = f(\ln U)$.

The result shown in Fig. 5 even exceeded all the expectations. In addition to the obvious overheating effect at high applied voltages, the CVC happened to be not only nonlinear, but even two-valued in its low voltage part. That is, the magnitude of the current flowing through the sample depended on the measurement protocol, had it been measured with increasing or with decreasing voltage.

The effect seems unusual and poorly described in the known literature. However, it is not completely new. For example, the lower branch arising with increasing voltage was observed and received its explanation in [15] where rise in R with increasing U in a low voltage range is supposed to be due to the suppression of weak Josephson coupling between superconducting inclusions with increasing current. Perhaps the most complete experimental study of the non-thermal hysteresis of the current-voltage characteristics in superconductors with weak Josephson links using the example of thin vanadium superconducting films was carried out in little-known paper [16], where this effect has been comprehensively studied depending on the grain size, the degree of oxidation of the intergrain boundaries, the influence of the temperature, magnetic field and microwave radiation. The paper emphasizes that the observed effect is related to the dynamics of the destruction of superconductivity by current in a superconducting network with weak (Josephson) links, and one can well expect its

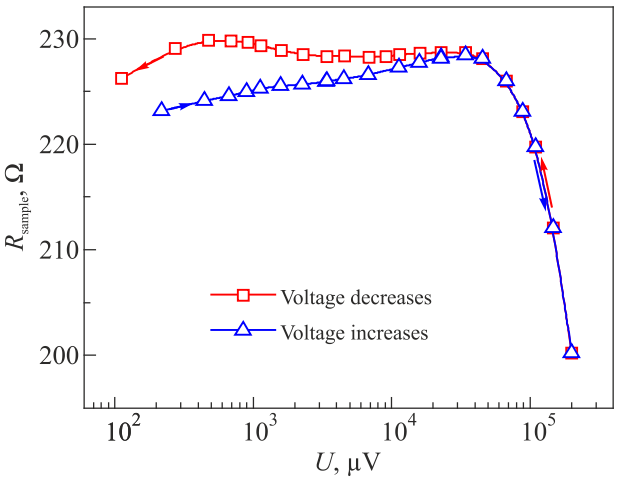

Fig. 5. (Color online) Resistance R as a function of applied voltage U at $T = 4.2$ K for Eu_A sample.

existence in any spatially inhomogeneous superconducting systems with percolation current flow.

For the HTSC similar effect has also been observed [17] and for Gd-based ruthenocuprates almost the same mechanism led to the appearance of stepwise structure in MR curves [18].

Thus, we can conclude that at the selected measuring current I = 100 μA for the samples subjected to a long-term storage, the superconducting state in the intergranular percolation network is suppressed by supercritical current and the weak Josephson intergranular links are in a normal state. And in order to see what remains in the samples after the superconductivity is destroyed, we will return to the comparison of the temperature dependence of the resistance for the initially prepared and the aged samples. But now we compare them in semi-logarithmic plot.

3.4. Low-temperature resistance comparison

In such a representation shown in Fig. 6 that allows us to emphasize the low-temperature data, we can clearly see that the peculiarities in ρ(T) behavior for the freshly prepared (Figs. 6(a), (b) and the aged Fig. 6(c)) samples remarkably coincide.

Because the superconducting interior of each grain in aged ceramic samples is hidden under a sufficiently thick shell of a disordered oxygen-deficient substance with a lowered T_c, the intragranular superconducting transitions are hardly visible in the ρ(T) dependencies for the samples subjected to aging.

With a further decrease in temperature, the superconducting transitions occurring in the oxygen-deficient disordered superconducting substance that covers the surface of $RuSr_2(Eu_{1.5}Ce_{0.5})Cu_2O_{10}$ granules are expressed on the temperature dependences of the intergranular hopping resistivity for the aged samples Eu_A and Eu_B in the form of a jump-like increases in resistance.

For example, at the temperature T_{c0} = 19.2 K that corresponds to establishing of intergranular superconductivity in oxygen-saturated sample Eu_B for the same sample after 10 years of storage we can see a characteristic jump in the ρ(T) dependence. And a similar jump at T_{c0} = 10 K, however, less pronounced, is also visible for sample Eu_A with lower oxygen content than for sample Eu_B.

This effect is obviously associated with a decrease in the density of normal electrons, after some of them are eliminated from the processes of hopping conductivity, forming a superconducting condensate.

But the most remarkable feature for the aged samples is the strictly logarithmically increasing resistance (see Fig. 7) following this intergranular superconducting transition with decreasing temperature, which extends to the lowest temperatures reached in our experiment. This logarithmic growth is apparently not related to superconductivity, since, according to Fig. 5 and the explanations in Sec. 3.3, the superconducting state in our aged samples is suppressed by the

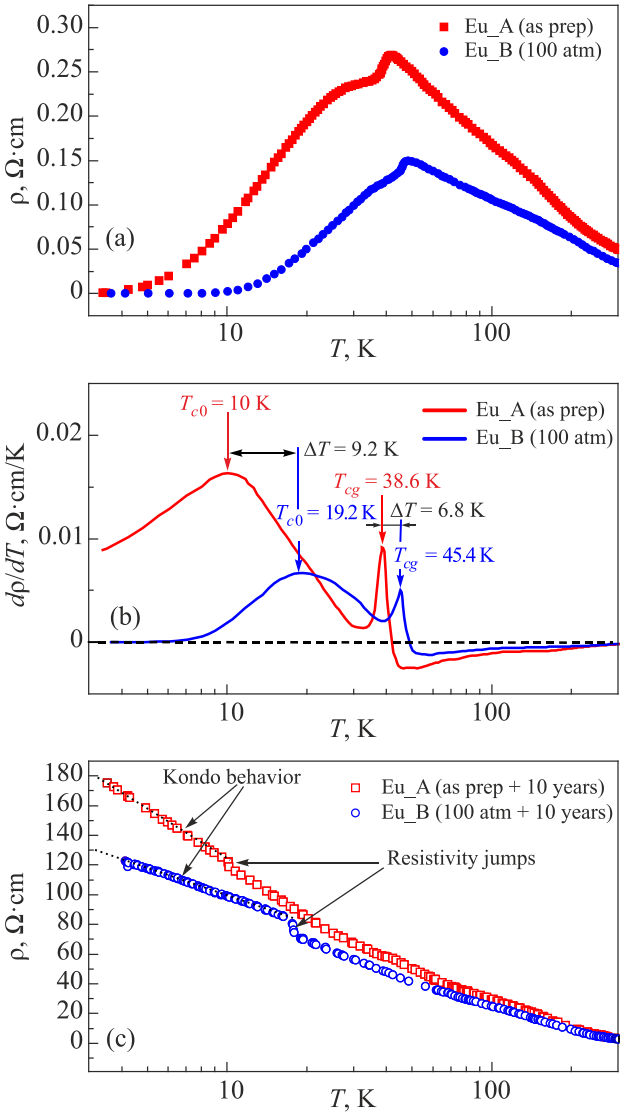

Fig. 6. (Color online) Low-temperature resistance behavior for the as prepared and the 10 year aged samples.

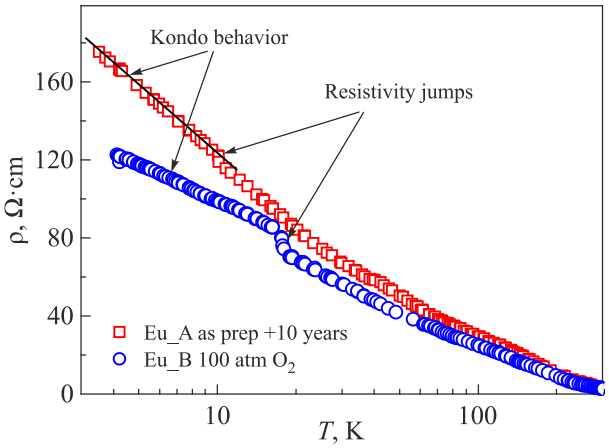

Fig. 7. Logarithmic grows of resistance for the aged Eu_A and Eu_B samples.

measuring current I = 100 μA flowing through the sample. Thus, the disordered shells of ruthenocuprate granules which were formed as a result of oxygen loss must be in the state of a normal metal with suppressed superconductivity.

There are several variants of localization corrections with a logarithmic temperature dependence of resistance. These are the 2D effects of weak localization and electron–electron interaction (EEI) [19] and a 3D Kondo effect [20]. It is obvious that the effects of weak localization of electrons cannot be realized in ferromagnets, which are the ruthenocuprate samples studied. Thus, there left two options: 2D effects EEI and a 3D Kondo effect.

The effects of EEI seem to be the most natural explanation for the observed logarithmic behavior, but their manifestation requires the presence of a 2D metal layer. Such a layer, indeed, can be formed on the surface of ruthenocuprate granules when the weak superconductivity in the oxygen-depleted disordered substance is suppressed by the measuring current applied to the sample. It remains, however, incomprehensible why such a logarithmic dependence has not been observed for the other non-magnetic granular HTSCs parental to ruthenocuprates. For example, for very thoroughly studied compounds, such as YBaCuO, which are also prone to the loss of stoichiometric oxygen and to formation of oxygen-depleted layers on the surface of the granules.

In addition, as it will be shown later, the observed effect has rather pronounced magnetic field dependence with positive magnetoresistance, which is not characteristic of EEI effects.

The assumption about the possibility of implementation the Kondo effect looks more “exotic”. The Kondo effect is usually associated with the presence of small quantities of paramagnetic impurities in a 3D metal, but Kondo lattices of localized paramagnetic ions that experience antiferromagnetic exchange interaction with conduction electrons are also known [21,22]. And even more than that, in recent years there have been many works (mainly theoretical) on the possibility of the manifestation of the Kondo effect in Ce-based antiferromagnets and even in weak ferromagnets [23] and [24]. These theoretical constructs are based on a so-called “underscreened” Kondo model where coexistence between the Kondo effect and the magnetic order is obtained. The competition between the Kondo effect on each atom, which tends to suppress the magnetic moment with decreasing temperature and leads to the Kondo temperature $T_K \propto \exp\left(-1/|J\rho|\right)$ and the RKKY interaction, which, on the contrary, tends to give a magnetic ordering between different magnetic atoms with the Neel temperature $T_N \propto |J\rho|^2$ is described by the well-known “Doniach diagram” [25].

And there are also some experimental papers, in which the Kondo effect was observed in some magnetically ordered uranium [26], ytterbium [27] and cerium [28] compounds.

It should also be noted that the Kondo effect is usually associated with the appearance of the Kondo characteristic temperature T_K, which is usually interpreted as the temperature of the resistance minimum, in a metal with paramagnetic impurities. This minimum is formed as a result of competition between the contributions of various electron scattering mechanisms (for example electron-phonon scattering), that lead to an increase in the metal resistance for $T > T_K$ and an increase in the exchange interaction constant between the spins of conduction electrons and the spins of paramagnetic impurities at $T < T_K$, leading to a logarithmic increase in resistance with decreasing temperature.

Of course, in our case, for a granulated ceramic system, in which electron transfer is determined not by phonon or magnon scattering, but by 3D VRH hopping conductivity, the appearance of a resistance minimum is impossible. At the same time, for the oxygen-deficient disordered shells covering ruthenocuprate granules after their transition to superconducting state with decreasing temperature and subsequent transition to metallic state by critical current, the spin logarithmic contribution to the resistance may take place.

Thus, a hypothesis arises about the possible manifestation of the Kondo effect in a metalized oxygen-deficient magnetic Josephson medium covering the $RuSr_2(Eu_{1.5}Ce_{0.5})Cu_2O_{10}$ granules on the background of weak superconductivity destroyed by the supercritical current.

Having studied in detail the temperature dependences of resistance, we can now turn to the study of magnetic field dependences of resistance, which sometimes provide more information for studying insulator–metal–superconductor transitions in granular media [29].

3.5. Magnetoresistance

It is known that the application of an external magnetic field suppresses superconductivity. Figure 8 shows the magnetoresistance behavior for the sample Eu_B (saturated with oxygen) in initial state and after 10 years of storage. We can see that in the temperature range of the intergra-

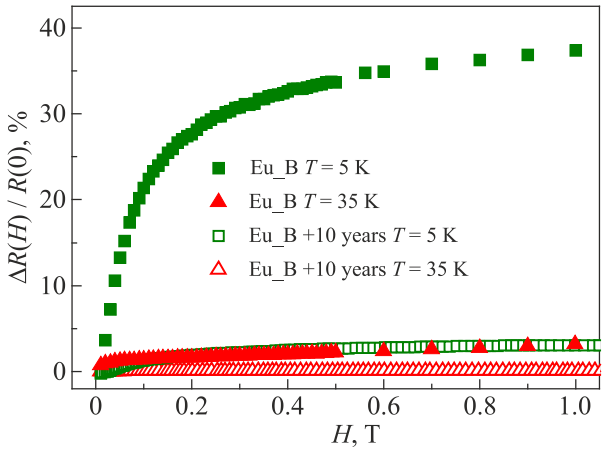

Fig. 8. (Color online) Magnetoresistance for the sample Eu_B with different oxygen content.

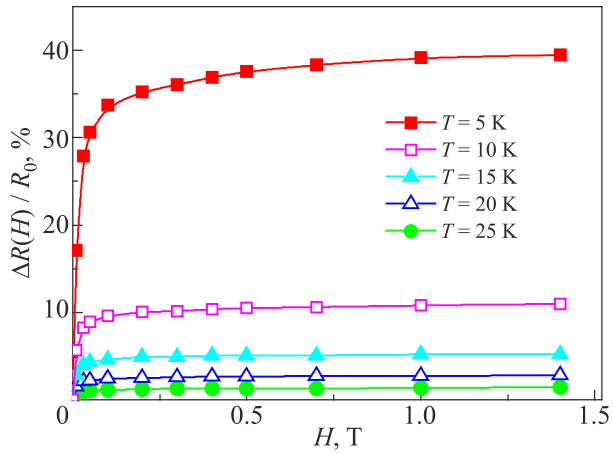

Fig. 9. Low temperature magnetoresistance for the most oxygen saturated sample Eu_B after preparation at 100 atm O_2.

nular superconducting transition (T = 5 K) for the sample saturated with oxygen, the magnetoresistance is positive and reaches 35% in magnetic field H = 1 T. At the temperature T = 35 K, it still remains positive, but does not exceed 3%. This corresponds to the reports [4] on huge upper critical fields H_{c2} ~ 80 T for intragranular superconductivity in ruthenocuprates. After the oxygen loss for the sample Eu_B at T = 5 K, the magnetoresistance falls down to the level of < 3%, and at T = 35 K it tends to zero. Such magnetoresistance drop is quite usual for a granular superconductor losing oxygen.

In "finer details", the magnetoresistance curves taken for different temperatures are shown in Figs. 9 and 10.

The dependences of the magnetoresistance at different temperatures are complex. For initially prepared sample Eu_B (the most saturated with oxygen) the magnetoresistance curves reach saturation, as would be expected for any granular superconductor with a high intragranular upper critical field and weak superconductivity in Josephson links between granules. For the aged sample Eu_A (the most oxygen depleted) we can see how the positive magnetoresistance decreases with growing temperature and maxima appear on the curves.

This form of magnetoresistive curves (with maximum) for oxygen-deficient magnetic superconductors, may reflect the competition between positive magnetoresistance associated with suppression of the remnants of weak superconductivity in the intergranular Josephson medium by the applied magnetic field and negative magnetoresistance associated with increased magnetic ordering in a weak ferromagnetic ruthenocuprate material which has already undergone a transition to the state of the nonsuperconducting metal.

With a further increase in temperature (Fig. 11) the positive magnetoresistance increases again, reaches a new maximum near the temperature of the intragranular superconducting transition, and then decline, changing sign and going into the region of negative values. This new burst of positive magnetoresistance is apparently associated with the suppression of the remnants of high-temperature superconductivity in the granules' inner cores, while the negative magnetoresistance is generally characteristic of substances with hopping conductivity and often witnessed a metal-insulator transition [29]. As a rule, it is caused by the effect of the orbital shrinking of the electron wave functions [30]. With further increase in temperature up to T = 300 K, this negative magnetoresistance decreases almost to zero.

A detailed quantitative analysis of the behavior of magnetoresistance is beyond the scope of this article. For our purposes, we can only note that the magnetoresistance behavior confirms the presence of both intragranular and intergranular superconducting transitions in ruthenocuprate samples depleted in oxygen after long storage and the metal-insulator transition that accompanies them.

The entire picture of magnetoresistance behavior in the whole temperature range is shown in Fig. 12 as values of resistance changes in magnetic fields H = 1.0 T and H = 0.5 T where points corresponds to different magnetoresistive curves, while lines are only guides to the eye.

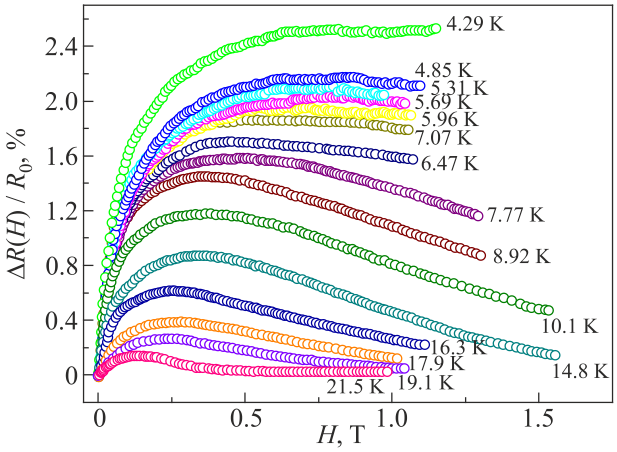

Fig. 10. (Color online) Low temperature magnetoresistance for the most oxygen deficient sample Eu_A after 10 years of storage.

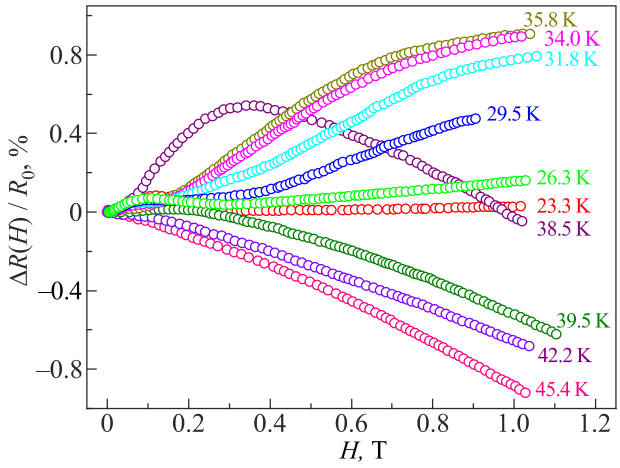

Fig. 11. (Color online) Magnetoresistance of Eu_A sample at some temperatures in the vicinity of intragranular superconducting transition.

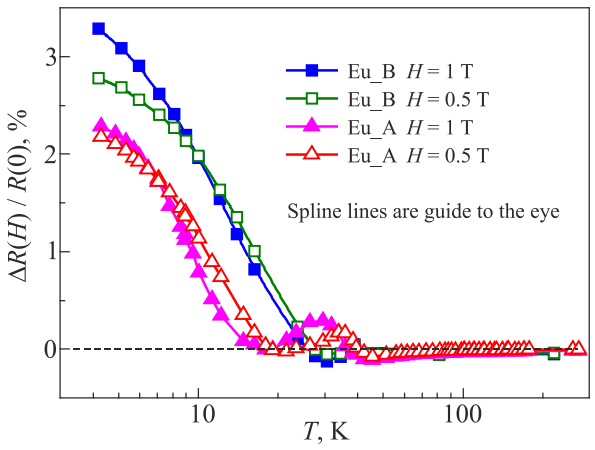

Fig. 12. (Color online) The whole picture of resistance changes (values and signs) for Eu_A and Eu_B samples in magnetic fields H = 1.0 T and H = 0.5 T, applied to the samples.

4. Conclusion

Superconductivity in ruthenocuprate samples subjected to a long-term storage is weakened, localized, percolation in nature and does not embrace the entire sample. In an intergranular medium, it is easily suppressed by a rather weak magnetic field or a measuring current (I = 100 μA).

Hysteresis due to the movements of N–S boundaries in a Josephson medium with weakened superconductivity under the influence of a changing current leads to the manifestation of hysteresis on the current-voltage characteristics (Fig. 5).

The studying of the temperature dependencies of resistance at high temperatures reveals two areas of manifestation of 3D variable range hopping Mott's conductivity and, on this basis, leads to conclusion about the granular structure of the sample.

This conclusion is confirmed by both electron microscopy data and the "shoulder-like" structure of superconducting transitions, which makes it possible to determine the temperatures of intragranular and intergranular superconductivity for the initially prepared samples.

For our samples, after they have lost oxygen as a result of 10 years of storage in ambient atmosphere, the ρ(T) dependences have some features that coincide in temperature with the temperatures of the intergranular and intragranular superconducting transitions and with the temperature of the magnetic AFM–WFM transition for the initially prepared samples.

At the same temperatures, for our oxygen-deficient samples, a change in the magnitude and sign of magnetoresistance is observed. The temperature behavior of magnetoresistance corresponds to the general picture of intragranular and intergranular superconducting transitions and a change in its sign witnessed a metal–insulator transition in granular samples.

The constancy of AFM–WFM transition temperature suggests the constancy of the oxygen content in the octahedral environments of magnetic Ru^{5+} ions. Thus, it can be assumed that the oxygen loss takes place in $(Ce_x\text{-}Eu_{2-x})$–O_2 "fluorite blocks" being "dielectric spacers" between the magnetic RuO layers and the superconducting layers CuO and is associated with the variable valence of Ce.

The observed invariance of temperatures for intragranular and intergranular superconductivity in the initially prepared samples and in the same samples after a partial loss of oxygen as a result of long-term storage indicates that the superconducting regions decrease in size, but retain their previous composition. This leads to the fact that both VRH hopping conductivity and superconductivity begin to acquire a percolation character.

The large difference for the superconducting transition temperatures corresponding to the intragranular and intergranular superconductivity, and invariability of these temperatures in the samples after long-term storage, suggests that the intragranular and intergranular substances have different phase composition. Presumably it could be $RuSr_2(Eu_{1.5}Ce_{0.5})Cu_2O_{10-\delta}$ for intragranular and $RuSr_2GdCu_2O_{8-\delta}$ for intergranular substance.

The logarithmic increase in resistance with decreasing temperature after the destruction of superconductivity in an intergranular medium by a supercritical current is the most unexpected phenomenon.

It can be explained either as the behavior of a dirty two-dimensional metal on the surface of granules in which electron-electron interaction processes predominate, or it may be interpreted as a manifestation of the Kondo effect in a normal metal with magnetic impurities.

It is difficult to make a final conclusion based on the measurements performed in this work, however, the presence of a positive magnetoresistance in the region where the logarithmic temperature dependence shown in Fig. 6 takes place gives an argument in favor of the Kondo effect (although this positive magnetoresistance can also be associated with the suppression of residual superconductivity by an applied magnetic field).

Of the studies that may be related to the problem of the Kondo effect in ruthenocuprates, one should also mention the increase in electronic heat capacity by the Schottky-type anomaly that was observed in gadolinium based ruthenocuprates and the observation of the "crossing-point effect" in the behavior of specific heat measured at different values of applied magnetic field [31] which is supposed to be inherent for strongly correlated electron systems.

It should also be noted that Kondo effect is essentially an interaction between a localized spin moments and itinerant electrons. And then we can suppose that there is a competition between itinerant and ion magnetism in ruthenocuprates. And in this picture the superconducting transition in magnetic environment means achievement of their equilibrium. In this case, after the destruction of weak intergra-

nular superconductivity under the influence of a critical current, we could indeed observe a logarithmic increase in conductivity associated with the manifestation of the Kondo effect.

An additional argument in favor of the Kondo effect is the fact that a logarithmic increase in resistance with decreasing temperature has not been observed in closely related to ruthenocuprates non-magnetic HTSCs compounds of $YBa_2Cu_3O_{7-\delta}$ type. Thus, the observed effect is clearly associated with magnetism.

In conclusion, the authors would like to express their deep gratitude to Professor D.G. Naugle of Texas A&M University for the ruthenocuprate samples given for the measurements and for the valuable scientific instruments donated to our laboratory by the Texas A&M University, as well as to our friend and teacher Dr. B.I. Belevtsev, whose ideas formed the basis for this article.

1. I. Felner, U. Asaf, Y. Levi, and O. Millo, *Physica C* **334**, 141 (2000).
2. G.V.M. Williams and M. Ryan, *Phys. Rev. B* **64**, 094515 (2001).
3. A. Shengelaya, R. Khasanov, D.G. Eschenko, I. Felner, U. Asaf, I.M. Savić, H. Keller, and K.A. Müller, *Phys. Rev. B* **69**, 024517 (2004).
4. T. Nachtrab, Ch. Bernhard, Ch. Lin, D. Koelle, and R. Kleiner, *Comptes Rendus Physique* **7**, 68 (2006).
5. I. Felner, *Coexistance of Superconductivity and Magnetism in* $R_{2-x}Ce_xRuSr_2Cu_2O_{10-\delta}$ (R = Eu and Gd), *arXiv:cond-mat/0211533*.
6. P.W. Klamut, *Supercond. Sci. Technol.* **21**, 093001 (2008).
7. S.G. Ovchinnikov, *Usp. Fiz. Nauk* **173**, 27 (2003).
8. P.W. Klamut, *PMC Physics B* **3**, 2 (2010).
9. B.D. Hennings, K.D.D. Rathnayaka, D.G. Naugle, and I. Felner, *Physica C* **370**, 253 (2002).
10. I. Felner, U. Asaf, Y. Levi, and O. Millo, *Phys. Rev. B* **55**, R3374 (1997).
11. V.V. Derevyanko, T.V. Sukhareva, and V.A. Finkel, *Solid State Phys.* **59**, 1492 (2017).
12. N.F. Mott, *J. Non-Cryst. Solids* **1**, 1 (1968).
13. T. Jarlborg, *Helvetica Physica Acta* **61**, 421 (1988).
14. V.B. Krasovitsky, B.I. Belevtsev, E.Yu. Beliayev, D.G. Naugle, K.D.D. Rathnayaka, and I. Felner, *J. Phys. Conf. Ser.* **51**, 283 (2006).
15. B.I. Belevtsev, N.V. Dalakova, and A.S. Panfilov, *Physica C* **282–287**, 1223 (1997).
16. О.Г. Туртанов, *Вісник Запорізького національного університету*, № 3, 265 (2015).
17. M.I. Petrov, D.A. Balaev, D.M. Gokhfeld, K.A. Shaikhutdinov, and K.S. Alexandrov, *Solid State Phys.* **44**, 1229 (2002).
18. B.I. Belevtsev, E.Yu. Beliayev, D.G. Naugle, and K.D.D. Rathnayaka, *Physica C* **483**, 186 (2012).
19. I.V. Gornyi and A.D. Mirlin, *Phys. Rev. B* **69**, 045313 (2004).
20. V.Yu. Irkhin, *Phys.-Usp.* **60**, 747 (2017).
21. V.V. Moshchalkov and N.B. Brandt, *Sov. Phys. Usp.* **29,** 725 (1986).
22. A.A. Abrikosov, *Sov. Phys. Usp.* **12**, 168 (1969).
23. Yu.P. Irkhin and V.Yu. Irkhin, *Electronic Structure, Physical Properties and Correlation Effects in d- and f-metals and their Compounds*, Regular and Chaotic Dynamics, Institute for Computer Research (2008) (in Russian).
24. B. Coqblin, M.D. Núñez-Regueiro, A. Theumann, J.R. Iglesias, and S.G. Magalhães, *Philos. Mag.* **86**, 2567 (2006).
25. S. Doniach, *Physica B+C* **91**, 231 (1977).
26. Schoenes, *J. Less Common Metals* **121**, 87 (1986).
27. K. Alami-Yadri, H. Wilhelm, and D. Jaccard, *Physica B* **259–261**, 157 (1999).
28. T. Graf, J.D. Thompson, M.F. Hundley, R. Movshovich, Z. Fisk, D. Mandrus, R.A. Fischer, and N.E. Phillips, *Phys. Rev. Lett.* **78**, 3769 (1997).
29. B.I. Belevtsev, E.Yu. Beliayev, Yu.F. Komnik, and E.Yu. Kopeichenko, *Physica B* **254**, 260 (1998).
30. B.I. Shklovskii and B.Z. Spivak, in: *Hopping Transport in Solids*, M. Pollak and B. Shklovskii (eds.), Elsevier, Amsterdam (1991), p. 271.
31. B.I. Belevtsev, V.B. Krasovitsky, D.G. Naugle, K.D.D. Rathnayaka, G. Agnolet, and I. Felner, *Bulletin of the Russian Academy of Sciences: Physics* **74**, 1049 (2010).

Взаємовплив стрибкової провідності та надпровідності у зразках магнітного надпровідника $RuSr_2(Eu_{1,5}Ce_{0,5})Cu_2O_{10-\delta}$

Є.Ю. Біляєв, В.О. Горєлий, Ю.О. Колесніченко

Проаналізовано температурні залежності опору та магнітоопору двох керамічних зразків $RuSr_2(Eu_{1,5}Ce_{0,5})Cu_2O_{10-\delta}$, один з яких залишено у початковому стані, а інший насичено киснем. Вимірювання на зразках виконано незабаром після приготування та повторено після тривалого зберігання (10 років) у навколишній атмосфері, коли вони втратили більшу частину свого надстехіометрічного та частину стехіометрічного кисню. Вивчено максимально широкий діапазон концентрацій кисню та зроблено спробу з'ясувати не тільки питання стабільності надпровідного стану в рутенокупратах, але й взаємодію різних типів електронної стрибкової провідності та надпровідності у гранульованому магнітному матеріалі. Незважаючи на значний прогрес, досягнутий в розумінні властивостей невпорядкованих провідників, питання взаємовпливу та конкуренції між локалізацією та надпровідністю досі не з'ясоване. Дослідження властивостей електронного транспорту при наближенні до переходу метал–ізолятор буде корисним та важливим.

Ключові слова: рутенокупрати, феромагнетизм, стрибкова провідність, надпровідність.

Взаимовлияние прыжковой проводимости и сверхпроводимости в образцах магнитного сверхпроводника $RuSr_2(Eu_{1,5}Ce_{0,5})Cu_2O_{10-\delta}$

Е.Ю. Беляев, В.А. Горелый, Ю.А. Колесниченко

Проанализированы температурные зависимости сопротивления и магнитосопротивления двух керамических образцов $RuSr_2(Eu_{1,5}Ce_{0,5})Cu_2O_{10-\delta}$, один из которых оставлен в исходном состоянии, а другой насыщен кислородом. Измерения на образцах были выполнены вскоре после приготовления и повторены после длительного хранения (10 лет) в окружающей атмосфере, когда они потеряли большую часть своего сверхстехиометрического и части стехиометрического кислорода. Изучен максимально широкий диапазон концентраций кислорода и сделана попытка выяснить не только вопросы стабильности сверхпроводящего состояния в рутенокупратах, но и взаимодействие различных типов электронной прыжковой проводимости и сверхпроводимости в гранулированном магнитном материале. Несмотря на значительный прогресс, достигнутый в понимании свойств неупорядоченных проводников, вопрос взаимного влияния и конкуренции между локализацией и сверхпроводимостью до сих пор не ясен. Исследование свойств электронного транспорта при приближении к переходу металл–изолятор будет полезным и важным.

Ключевые слова: рутенокупраты, ферромагнетизм, прыжковая проводимость, сверхпроводимость.